Research Article | Vol. 25, No. 4 | 20 Feb 2017 | OPTICS EXPRESS 3646

Optics EXPRESS

Gouy phase shift for annular beam profiles in attosecond experiments

F. SCHLAEPFER,[1,2,*] A. LUDWIG,[1,2] M. LUCCHINI,[1] L. KASMI,[1] M. VOLKOV,[1] L. GALLMANN,[1] AND U. KELLER[1]

[1]*Department of Physics, ETH Zurich, 8093 Zurich, Switzerland*
[2]*These authors contributed equally to this work.*
**f.schlaepfer@phys.ethz.ch*

Abstract: Attosecond pump-probe measurements are typically performed by combining attosecond pulses with more intense femtosecond, phase-locked infrared (IR) pulses because of the low average photon flux of attosecond light sources based on high-harmonic generation (HHG). Furthermore, the strong absorption of materials at the extreme ultraviolet (XUV) wavelengths of the attosecond pulses typically prevents the use of transmissive optics. As a result, pump and probe beams are typically recombined geometrically with a center-hole mirror that reflects the larger IR beam and transmits the smaller XUV, which leads to an annular beam profile of the IR. This modification of the IR beam can affect the pump-probe measurements because the propagation that follows the reflection on the center-hole mirror can strongly deviate from that of an ideal Gaussian beam. Here we present a detailed experimental study of the Gouy phase of an annular IR beam across the focus using a two-foci attosecond beamline and the RABBITT (reconstruction of attosecond beating by interference of two-photon transitions) technique. Our measurements show a Gouy phase shift of the truncated beam as large as 2π and a corresponding rate of 50 as/mm time delay change across the focus in a RABBITT measurement. These results are essential for attosecond pump-probe experiments that compare measurements of spatially separated targets.

OCIS codes: (320.7100) Ultrafast measurements; (320.7120) Ultrafast phenomena; (020.4180) Multiphoton processes; (300.6530) Spectroscopy, ultrafast.

References and links

1. F. Krausz and M. Ivanov, "Attosecond physics," Rev. Mod. Phys. **81**(1), 163–234 (2009).
2. L. Gallmann, C. Cirelli, and U. Keller, "Attosecond Science: Recent Highlights and Future Trends," Annu. Rev. Phys. Chem. **63**(1), 447–469 (2012).
3. A. L. Cavalieri, N. Müller, T. Uphues, V. S. Yakovlev, A. Baltuška, B. Horvath, B. Schmidt, L. Blümel, R. Holzwarth, S. Hendel, M. Drescher, U. Kleineberg, P. M. Echenique, R. Kienberger, F. Krausz, and U. Heinzmann, "Attosecond spectroscopy in condensed matter," Nature **449**(7165), 1029–1032 (2007).
4. S. Haessler, B. Fabre, J. Higuet, J. Caillat, T. Ruchon, P. Breger, B. Carré, E. Constant, A. Maquet, E. Mével, P. Salières, R. Taïeb, and Y. Mairesse, "Phase-resolved attosecond near-threshold photoionization of molecular nitrogen," Phys. Rev. A **80**(1), 011404 (2009).
5. M. Schultze, M. Fiess, N. Karpowicz, J. Gagnon, M. Korbman, M. Hofstetter, S. Neppl, A. L. Cavalieri, Y. Komninos, T. Mercouris, C. A. Nicolaides, R. Pazourek, S. Nagele, J. Feist, J. Burgdörfer, A. M. Azzeer, R. Ernstorfer, R. Kienberger, U. Kleineberg, E. Goulielmakis, F. Krausz, and V. S. Yakovlev, "Delay in photoemission," Science **328**(5986), 1658–1662 (2010).
6. K. Klünder, J. M. Dahlström, M. Gisselbrecht, T. Fordell, M. Swoboda, D. Guénot, P. Johnsson, J. Caillat, J. Mauritsson, A. Maquet, R. Taïeb, and A. L'Huillier, "Probing single-photon ionization on the attosecond time scale," Phys. Rev. Lett. **106**(14), 143002 (2011).
7. C. Palatchi, J. M. Dahlström, A. S. Kheifets, I. A. Ivanov, D. M. Canaday, P. Agostini, and L. F. DiMauro, "Atomic delay in helium, neon, argon and krypton," J. Phys. At. Mol. Opt. Phys. **47**(24), 245003 (2014).
8. D. Guénot, D. Kroon, E. Balogh, E. W. Larsen, M. Kotur, M. Miranda, T. Fordell, P. Johnsson, J. Mauritsson, M. Gisselbrecht, K. Varjù, C. L. Arnold, T. Carette, A. S. Kheifets, E. Lindroth, A. L'Huillier, and J. M. Dahlström, "Measurements of relative photoemission time delays in noble gas atoms," J. Phys. At. Mol. Opt. Phys. **47**(24), 245602 (2014).
9. M. Sabbar, S. Heuser, R. Boge, M. Lucchini, T. Carette, E. Lindroth, L. Gallmann, C. Cirelli, and U. Keller, "Resonance Effects in Photoemission Time Delays," Phys. Rev. Lett. **115**(13), 133001 (2015).
10. S. Heuser, Á. Jiménez Galán, C. Cirelli, C. Marante, M. Sabbar, R. Boge, M. Lucchini, L. Gallmann, I. Ivanov,

#283405 https://doi.org/10.1364/OE.25.003646
Journal © 2017 Received 22 Dec 2016; revised 2 Feb 2017; accepted 8 Feb 2017; published 10 Feb 2017

Optics EXPRESS

A. S. Kheifets, J. M. Dahlström, E. Lindroth, L. Argenti, F. Martín, and U. Keller, "Angular dependence of photoemission time delay in helium," Phys. Rev. A **94**(6), 063409 (2016).
11. J. Itatani, F. Quéré, G. L. Yudin, M. Yu. Ivanov, F. Krausz, and P. B. Corkum, "Attosecond streak camera," Phys. Rev. Lett. **88**(17), 173903 (2002).
12. M. Hentschel, R. Kienberger, C. Spielmann, G. A. Reider, N. Milosevic, T. Brabec, P. Corkum, U. Heinzmann, M. Drescher, and F. Krausz, "Attosecond metrology," Nature **414**(6863), 509–513 (2001).
13. P. M. Paul, E. S. Toma, P. Breger, G. Mullot, F. Augé, P. Balcou, H. G. Muller, and P. Agostini, "Observation of a Train of Attosecond Pulses from High Harmonic Generation," Science **292**(5522), 1689–1692 (2001).
14. H. G. Muller, "Reconstruction of attosecond harmonic beating by interference of two-photon transitions," Appl. Phys. B Lasers Opt. **74**(S1), 17–21 (2002).
15. L. Cattaneo, J. Vos, M. Lucchini, L. Gallmann, C. Cirelli, and U. Keller, "Comparison of attosecond streaking and RABBITT," Opt. Express **24**(25), 29060–29076 (2016).
16. M. Ossiander, F. Siegrist, V. Shirvanyan, R. Pazourek, A. Sommer, T. Latka, A. Guggenmos, S. Nagele, J. Feist, J. Burgdörfer, R. Kienberger, and M. Schultze, "Attosecond correlation dynamics," Nat. Phys. 3941 (2016).
17. R. Locher, L. Castiglioni, M. Lucchini, M. Greif, L. Gallmann, J. Osterwalder, M. Hengsberger, and U. Keller, "Energy-dependent photoemission delays from noble metal surfaces by attosecond interferometry," Optica **2**(5), 405–410 (2015).
18. M. Lucchini, L. Castiglioni, L. Kasmi, P. Kliuiev, A. Ludwig, M. Greif, J. Osterwalder, M. Hengsberger, L. Gallmann, and U. Keller, "Light-Matter Interaction at Surfaces in the Spatiotemporal Limit of Macroscopic Models," Phys. Rev. Lett. **115**(13), 137401 (2015).
19. M. Schultze, E. M. Bothschafter, A. Sommer, S. Holzner, W. Schweinberger, M. Fiess, M. Hofstetter, R. Kienberger, V. Apalkov, V. S. Yakovlev, M. I. Stockman, and F. Krausz, "Controlling dielectrics with the electric field of light," Nature **493**(7430), 75–78 (2012).
20. M. Schultze, K. Ramasesha, C. D. Pemmaraju, S. A. Sato, D. Whitmore, A. Gandman, J. S. Prell, L. J. Borja, D. Prendergast, K. Yabana, D. M. Neumark, and S. R. Leone, "Ultrafast dynamics. Attosecond band-gap dynamics in silicon," Science **346**(6215), 1348–1352 (2014).
21. M. Lucchini, S. A. Sato, A. Ludwig, J. Herrmann, M. Volkov, L. Kasmi, Y. Shinohara, K. Yabana, L. Gallmann, and U. Keller, "Attosecond dynamical Franz-Keldysh effect in polycrystalline diamond," Science **353**(6302), 916–919 (2016).
22. R. Locher, M. Lucchini, J. Herrmann, M. Sabbar, M. Weger, A. Ludwig, L. Castiglioni, M. Greif, M. Hengsberger, L. Gallmann, and U. Keller, "Versatile attosecond beamline in a two-foci configuration for simultaneous time-resolved measurements," Rev. Sci. Instrum. **85**(1), 013113 (2014).
23. L. G. Gouy, "Sur une propriété nouvelle des ondes lumineuses," C. R. Acad. Sci. Paris. **110**, 1251–1253 (1890).
24. Z. Chang, *Fundamentals of Attosecond Optics* (Taylor and Francis Group, LLC, 2011).
25. F. Lindner, G. G. Paulus, H. Walther, A. Baltuška, E. Goulielmakis, M. Lezius, and F. Krausz, "Gouy phase shift for few-cycle laser pulses," Phys. Rev. Lett. **92**(11), 113001 (2004).
26. N. Shivaram, A. Roberts, L. Xu, and A. Sandhu, "In situ spatial mapping of Gouy phase slip for high-detail attosecond pump-probe measurements," Opt. Lett. **35**(20), 3312–3314 (2010).
27. C. Cirelli, M. Sabbar, S. Heuser, R. Boge, M. Lucchini, L. Gallmann, and U. Keller, "Energy-Dependent Photoemission Time Delays of Noble Gas Atoms Using Coincidence Attosecond Streaking," IEEE J. Sel. Top. Quantum Electron. **21**(5), 1 (2015).
28. Z. Tao, C. Chen, T. Szilvási, M. Keller, M. Mavrikakis, H. Kapteyn, and M. Murnane, "Direct time-domain observation of attosecond final-state lifetimes in photoemission from solids," Science **353**(6294), 62–67 (2016).
29. S. Feng and H. G. Winful, "Physical origin of the Gouy phase shift," Opt. Lett. **26**(8), 485–487 (2001).
30. J. M. Dahlström, A. L'Huillier, and A. Maquet, "Introduction to attosecond delays in photoionization," J. Phys. At. Mol. Opt. Phys. **45**(18), 183001 (2012).
31. E. P. Wigner, "Lower Limit for the Energy Derivative of the Scattering Phase Shift," Phys. Rev. **98**(1), 145–147 (1955).

1. Introduction

To date most attosecond pump-probe measurements combine extreme-ultraviolet (XUV) attosecond pulses with a few-femtosecond phase-locked infrared (IR) pulse [1,2]. Fundamental fast processes such as photoemission can be resolved for the first time [3–10]. The most common techniques to unravel the attosecond dynamics are either based on attosecond streaking [11,12] or on RABBITT (Reconstruction of Attosecond Beating By Interference of Two-photon Transitions) [13,14]. However both measurement techniques only give access to relative time delays and have different trade-offs [15]. Relative photoemission time delays have been measured between two different initial states of the same target [5,6,16] or between different gas targets [8], for which better accuracy is obtained with coincidence measurements [9].

Optics EXPRESS

Alternatively, one can use a second spatially separated target to recalibrate the measurement and obtain absolute photoemission delays [17,18]. This approach makes it possible to study a wider range of ultrafast dynamics in gas, molecular and solid targets [19–21]. Depending on the kind of physical system under investigation, the target under test is either placed consecutively in close proximity to the reference target within the same focus [19–21] or spatially separated in a second focus using refocusing optics after a first focus for the reference target [Fig. 1] [22]. Such attosecond measurements would greatly benefit from more precise and more accurate temporal calibration below 10 attoseconds. This makes it essential to better understand the wavefront properties of the pump and probe beams along the spatially separated targets.

As a beam experiences a phase shift across the focus (Gouy phase shift) [23], the phase contribution introduced through the relative position of the targets within the focus becomes essential in phase-sensitive measurements. This phase shift directly impacts the measured time delay because phase and delay are linked via an energy derivative. One approach is to simply avoid the Gouy phase by placing the target sufficiently far away from the focus [13]. This also minimizes any possible averaging effect induced by a rapidly varying Gouy phase across the extended interaction volume probed in the experiment. For an ideal Gaussian beam, 50% of the total Gouy phase shift occurs within one Rayleigh range, with much slower phase evolution outside. However, in attosecond pump-probe experiments that combine the IR and the attosecond pulses geometrically, the IR beam can strongly deviate from a theoretical Gaussian shape. Such geometric beam combining is typically used because no suitable beamsplitters or dichroic optics are available for the XUV spectral region. A very common geometrical beam recombination scheme is to use a mirror with a center hole, for which the smaller XUV beam is transmitted through the center, while the larger IR beam is reflected on the outer mirror part. This produces an annular IR beam profile with a considerably different Gouy phase compared to an ideal Gaussian beam [24].

Previously it has been predicted by Chang [24] and measured by Lindner et al. [25] and Shivaram et al. [26] that the Gouy phase shift of a truncated few-cycle IR beam can be significantly larger than the π-shift of a Gaussian beam. Here, we used the RABBITT technique in a setup with two spatially separated foci to perform a detailed study of the Gouy phase shift of an annular IR beam produced by the reflection on a center-hole mirror. Our results show a Gouy phase shift of more than 2π and a corresponding rate of 50 as/mm time delay change across the focus in a RABBITT measurement. The result does not depend on the probing harmonic energy and shows that a precise calibration with a proper control of the target positions is mandatory in attosecond photoemission delay measurements with spatially separated targets. Our work demonstrates the feasibility of more precise attosecond pump-probe experiments, which can access absolute photoemission delays if combined with a proper choice of reference system.

2. Setup

A detailed description of the setup used in the experiment can be found in reference [22]. We used IR laser pulses with energy of up to 430 μJ, 25-fs time duration, a center wavelength of 790 nm and a pulse repetition rate of 1 kHz [Fig. 1]. A beamsplitter divides the IR beam into two parts. The strongest part (80%) of the IR beam is focused into a gas cell filled with argon for high-order harmonic generation (HHG). The emitted XUV spectrum consists of odd harmonics of the IR beam covering the energy range between 25 and 55 eV (harmonics 17 to 33). A 100-nm thick aluminum filter blocks the residual IR beam after HHG. The weaker part (20%) of the initial IR beam follows a delay path before being recombined with the XUV light on a center-hole mirror. The XUV beam propagates through the hole while the mirror reflects the IR beam. The combined collinearly propagating beams after the center-hole mirror are then focused with a toroidal mirror into the first reference target interaction chamber with a neon gas target and a time-of-flight spectrometer (ToF). After this first target,

Optics EXPRESS

a toroidal mirror makes a 1:1 image of the first focus into a second interaction chamber, which has also a neon gas target and a second ToF to fully characterize the absolute temporal accuracy of the setup.

The insets (a) and (b) in Fig. 1 show the beam profiles of the IR beam measured in the two foci. Inset (c) illustrates a cut through the second focus. It is clearly visible that the profile (red line) deviates strongly from a Gaussian fit (blue dashed line). The beam radius of the Gaussian fit is 47.9 µm, which would correspond to a Rayleigh length of 9.1 mm. The second gas target together with its ToF spectrometer can be moved along the beam propagation direction, which allows for RABBITT measurements over a propagation distance of 40 mm around the focus. The exact position of the IR beam focus in the second chamber has been determined by recording strong-field ionization yields from ethylene, a molecule with low ionization potential. If the few-femtosecond IR pulse is intense enough, the molecule is ionized via above-threshold-ionization (ATI). As shown in Fig. 2, the integrated ATI yield strongly depends on the *z*-position of the target. We determined the focus position of the IR beam at the maximum total electron yield. As we will see later, this point is in full agreement with the position where the Gouy phase goes through zero.

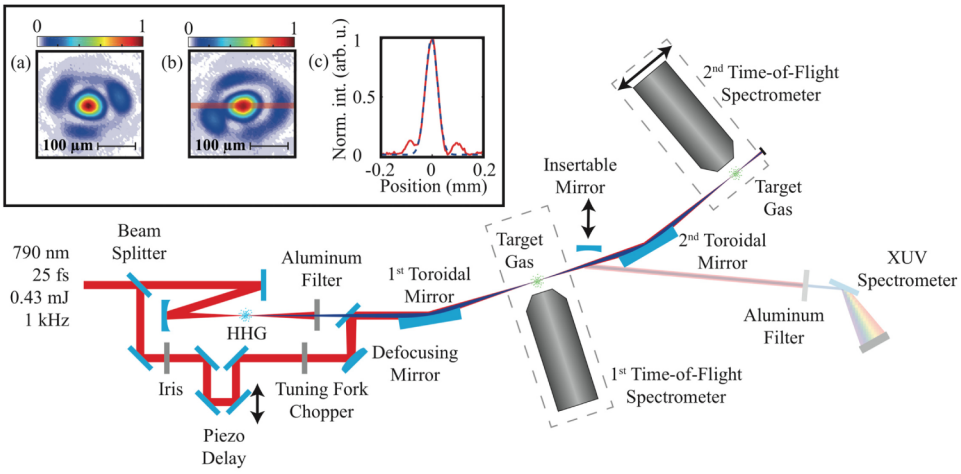

Fig. 1. Schematic of the two-target attosecond beamline with high-order harmonic generation (HHG), the attosecond/femtosecond interferometer and the two-foci geometry [22]. A defocusing mirror in the delay path matches the wavefronts of the IR and XUV on the center-hole mirror. The second gas target and time-of-flight (ToF) spectrometer can be moved together along the beam propagation direction. The insets (a) and (b) show the measured IR beam profile in the first (a) and second (b) focus. Inset (c) shows a cut of the second focus illustrated red in (b). The red curve is the beam profile and the blue dashed line a Gaussian fit.

Optics EXPRESS

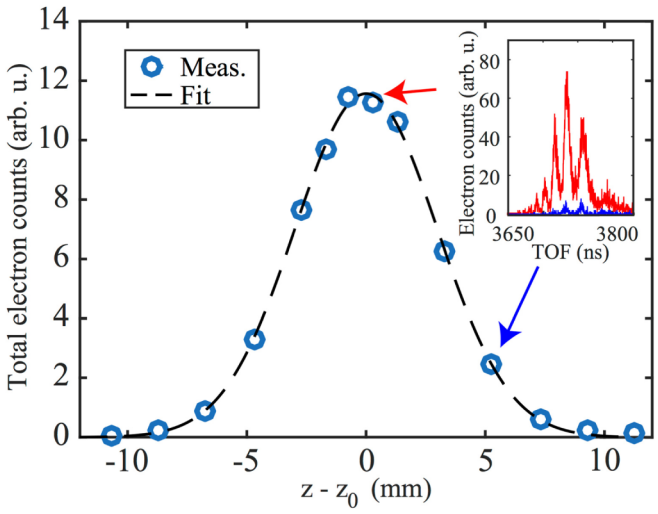

Fig. 2. Total measured electron counts of ATI spectra from ethylene as a function of the second chamber position (blue open dots) and the Gaussian fit (black dashed curve) used to extract the focal position. The inset shows two spectra for two positions of the second time-of-flight (ToF) spectrometer nozzle assembly, z = 0.25 mm (red arrow) and z = 5.25 mm (blue arrow).

3. Phase measurement

An example of two RABBITT traces recorded simultaneously in the two target regions is shown in Fig. 3. During the temporal overlap of the XUV pump and IR probe beam, oscillating sidebands appear in the photoelectron spectrum between the peaks, which originate from direct ionization via absorption of a harmonic photon. Each of these sidebands (SBs) is the result of the interference between two distinct two-photon, two-color ionization pathways. The sideband of order *2q* originates either from the absorption of a photon from the harmonic *2q-1* and an additional IR photon, or from the absorption of a photon from the harmonic *2q + 1* and the emission of one IR photon [13,14]. In the framework of the second-order perturbation theory, the SB oscillation can be described as follows:

$$SB_{2q}(\tau) \propto \cos(2\omega_{IR}\tau - \Phi_{2q}) = \cos(2\omega_{IR}\tau - \Delta\theta_{2q} - \Delta\varphi_{2q}^{At} + 2\varphi_{IR} + \varphi_0), \qquad (1)$$

where ω_{IR} is the IR frequency, τ is the pump-probe delay. Φ_{2q} is the total SB phase and corresponds to the phase directly measurable in the experiment. This total phase can be further decomposed into different terms: $\Delta\theta_{2q} = \theta_{2q+1} - \theta_{2q-1}$ is the phase difference between consecutive harmonics (attochirp), $\Delta\varphi_{2q}^{At}$ is the difference of the atomic phase contributions [9,15,27], φ_{IR} is the phase of the IR beam and φ_0 the arbitrary choice of the zero phase.

Usually the term of physical interest is the atomic term, since it is related to the photoionization process in the target under test. However here in our experiment we want to investigate how φ_{IR} changes along the focus. By using the same gas target in the two foci we assure that the atomic contribution is identical in the two interaction regions, $\Delta\varphi_{2q}^{At,(1)} = \Delta\varphi_{2q}^{At,(2)} = \Delta\varphi_{2q}^{Ne}$. We will show later that the effect of the refocusing mirror and the interaction in the first target on the phase of the XUV beam in the second target is negligible. Hence also the term $\Delta\theta_{2q}$ does not change between the two targets. The Gouy phase shift of the XUV beam can also be neglected due to its shorter wavelength (longer Rayleigh range).

Optics EXPRESS

It then follows that by changing the position of the second target along the IR beam focus we change mainly φ_{IR} due to the Gouy phase shift of the IR, $\varphi_{Gouy}^{IR}(z)$. By looking at the phase difference between two simultaneously acquired RABBITT traces we thus estimate the Gouy phase of the IR pulse (up to a constant offset):

$$\Delta\Phi_{2q}(z) = \Phi_{2q}^{(1)} - \Phi_{2q}^{(2)}(z) = 2\varphi_{Gouy}^{IR}(z) + \tilde{\varphi}_0, \quad (2)$$

where $\Phi_{2q}^{(1)}$ and $\Phi_{2q}^{(2)}(z)$ represent the phase extracted from the oscillation of the SB with order *2q* in the first and second ToF spectrum, respectively, and $\tilde{\varphi}_0$ is a constant phase offset due to the choice of target position in the first chamber.

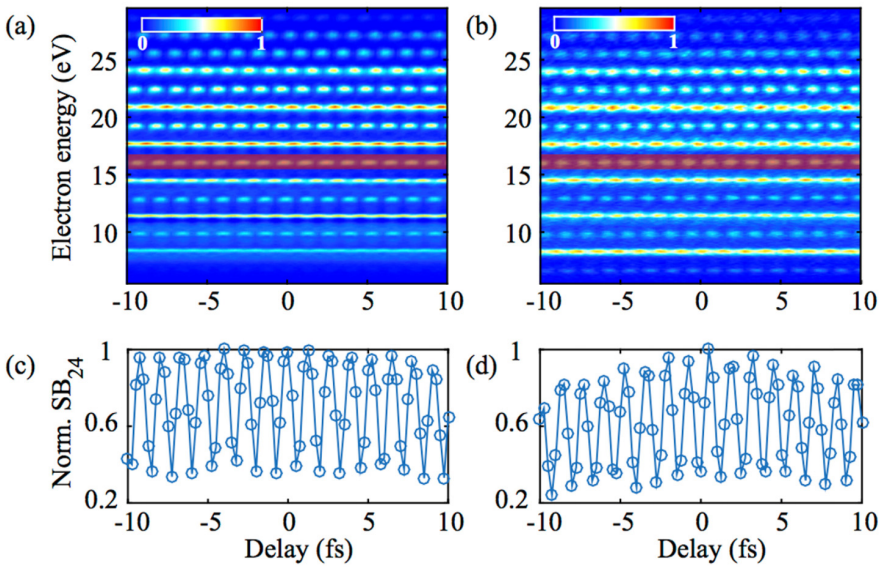

Fig. 3. (a), (b) Simultaneously measured RABBITT traces in the first and second Ne-target regions. Oscillating SBs with order 20 (9.82 eV) to 30 (25.52 eV) are clearly visible in both traces. (c), (d) Normalized electron yield of SB 24 obtained by integrating over the energy region highlighted in red in (a) and (b).

To extract $\Phi_{2q}(z)$ from the experimental traces we looked at the product between the Fourier transform of a particular SB signal in the first chamber [Fig. 3(c)], $\tilde{SB}_{2q}^{(1)}(\omega)$, and the complex conjugate of the same quantity extracted from the second ToF spectrum, $\tilde{SB}_{2q}^{(2)*}(\omega, z)$ (Fig. 3(d); for further details see supplementary material of [28]):

$$C_{2q}(\omega, z) = \tilde{SB}_{2q}^{(1)}(\omega) \cdot \tilde{SB}_{2q}^{(2)*}(\omega, z). \quad (3)$$

$\left|C_{2q}(\omega, z)\right|$ has a peak at the common oscillation frequency $\omega_0^{2q} \cong 2\omega_{IR}$ of the two traces and a corresponding phase that is equal to the phase difference between the two sideband signals, $\Delta\Phi_{2q}(z)$. We first calculated the average value of ω_0^{2q} over all the SB orders and found it to be $\omega_0^{avg} = 4.77 \pm 0.06$ PHz. Then we used Eq. (3) to evaluate $\Delta\Phi_{2q}(z)$ for each individual SB order at the frequency ω_0^{avg} in order to ensure that the extracted phase difference always corresponds to the same oscillation period. The Gouy phase $\varphi_{Gouy}^{IR}(z)$ corresponds to half of the extracted $\Delta\Phi_{2q}(z)$ apart from the arbitrary constant $\tilde{\varphi}_0$ [Eq. (2)].

Optics EXPRESS

In a first step, we investigated in detail the dependence of the phase difference $\Delta\Phi_{2q}(z)$ on the SB order *2q*. The main phase term that is expected to change between different SBs is the attochirp of the XUV, $\Delta\theta_{2q}$. Figure 4(a) shows the individual phases Φ_{2q} from the RABBITT oscillations extracted in the first (red circles) and in the second focus (blue circles, z = –2.7 mm) for each SB. The attochirp results in a significant change of the individual phases of more than 0.7π between SB 18 and 32. Nevertheless, one would expect the effect of the attochirp $\Delta\theta_{2q}$ to cancel out completely in $\Delta\Phi_{2q}(z)$ [Eqs (1) and (2)]. This is true if no significant distortion is induced in the harmonics by the refocusing toroidal mirror and if the variation of the Gouy phase of the XUV light with the harmonic order is negligible. To quantify this statement more precisely, we plot the relative phase difference $\Delta\Phi_{2q}(z)$ as a function of the SB order for several measurement points along the focus [Fig. 4(b)]. By comparing Fig. 4(a) with Fig. 4(b) we can show that taking the difference between the two target phases removes efficiently the attochirp. Therefore, we can conclude that the refocusing toroidal mirror in our two-foci setup does not introduce any energy-dependent delay on the harmonics. As a consequence, it is justified to assume an energy-independent propagation delay between the two spatially separated target regions. Furthermore, we can conclude that the attochirp is removed by taking the phase difference between the two spatially separated targets, independent from the exact position of the second target. The fact that we did not observe any energy dependence of the phase difference $\Delta\Phi_{2q}(z)$ also supports our assumption that the Gouy phase of each harmonic does not significantly affect the phase difference $\Delta\Phi_{2q}(z)$ and thus any spatial dependence of this quantity can be ascribed solely to the IR Gouy phase.

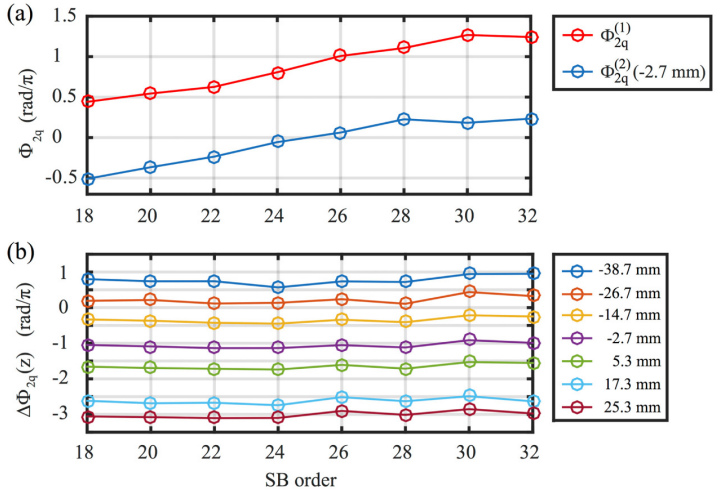

Fig. 4. (a) Energy dependence of the oscillation phase measured in the first and second target region (red = 1st, blue = 2nd). The phase has been extracted from eight SBs. Here, the position of the second target is z = –2.7 mm. The phase increases clearly in both foci with increasing SB energy as a result of the XUV attochirp. (b) Energy dependence of the relative phase difference, $\Delta\Phi_{2q} = \Phi_{2q}^{(1)} - \Phi_{2q}^{(2)}(z)$, for seven positions of the second target.

Figure 5(a) shows the extracted Gouy phase $\varphi_{Gouy}^{IR}(z)$ of the IR beam obtained with the method described above from eight different SB oscillations (orders 18-32). For all SBs, the phase experiences a change of almost 2π within a spatial range of –40 mm to 30 mm around the focus [Fig. 2], which exceeds by far the π–shift of an ideal Gaussian beam. The phase shifts extracted from different SBs are virtually indistinguishable. This confirms that there is

Optics EXPRESS

no appreciable dependence on the XUV wavelength as already indicated by our data shown in Fig. 4. Thus, we can average the phase behavior from different SBs for a better estimate of $\varphi_{Gouy}^{IR}(z)$. Figure 5(b) displays $\varphi_{Gouy}^{IR}(z)$ obtained by averaging over the SB orders for two independent measurements taken under identical experimental conditions on different days. The error bars represent the standard deviation within each data set. The two curves overlap perfectly, which confirms the reproducibility of the measurements.

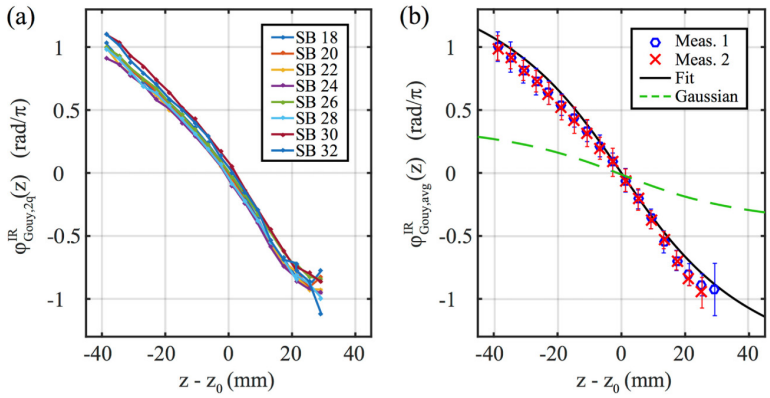

Fig. 5. (a) Phase difference between simultaneously measured RABBITT traces obtained for eight different sidebands while varying the position of the second interaction chamber. (b) Phase difference averaged over the SB orders for two independent measurement sets. The error bars represent the corresponding standard deviation. The black line is the result of a fit with the function $\varphi = -A \cdot \tan^{-1}(z/z_R)$, giving A = 2.45 ± 0.37 and z_R = 32.7 ± 6.8 mm. The green dashed line illustrates the Gouy phase of a Gaussian beam with the same Rayleigh length z_R.

The Gouy phase shift of an ideal Gaussian beam is described by $\varphi = -\tan^{-1}(z/z_R)$, with z_R denoting the Rayleigh length. According to Refs [24,29], the Gouy phase of an annular beam follows the arctan shape as well, but with an additional pre-factor $A \neq 1$, thus $\varphi = -A \cdot \tan^{-1}(z/z_R)$. If we use this expression to fit our data, we find A = 2.45 ± 0.37 and z_R = 32.7 ± 6.8 mm [Fig. 5(b)]. We can conclude as follows:

1) The Rayleigh length z_R is substantially larger than the one extracted from an ideal Gaussian fit of the IR beam profile (z_R = 9.1 mm). As shown in the setup description [Fig. 1] our IR beam reflected from a center-hole mirror deviates strongly from a Gaussian beam profile. Furthermore our IR beam experiences some astigmatism. As we demonstrated, the variation of the Gouy phase along the beam propagation direction z is still considerable even a few centimeters away from the focus.

2) The large pre-factor A shows clearly that the Gouy phase shift of a beam reflected on a center-hole mirror strongly deviates from the one of a beam with a Gaussian profile and cannot be simply neglected [Fig. 5(b)].

4. Equivalent photoionization delays

In attosecond pump-probe spectroscopy the spectral phase of an electron wave packet (EWP) contains time information about the system under test. In the photoemission process for example, the EWP experiences a phase offset depending on the initial state. The energy derivative of the phase corresponds to a group delay and therefore a relative phase offset between EWPs emitted from different initial states reveals directly the relative photoemission delay between them [5] as long as the continuum does not contain any resonances [9]. As the SB phase of a RABBITT measurement corresponds to a sum of phase differences [Eq. (1)], it is possible to directly obtain the photoemission delay associated with the two-color, two-

Optics EXPRESS

photon ionization process [30] in the framework of the finite difference approximation as follows:

$$\tau_{2q} = \frac{\partial \Phi_{2q}}{\partial \omega} \cong \frac{\Phi_{2q}}{2\omega_{IR}} = \tau_{2q,chirp} + \tau_{2q,atom} - \tau_{IR} - \tau_0. \quad (4)$$

$\tau_{2q,chirp}$ is the group delay of the XUV (attochirp), $\tau_{2q,atom}$ is the atomic delay consisting of the Wigner delay and the continuum-continuum delay [30,31], τ_{IR} is the delay resulting from the IR phase and the constant τ_0 results from the arbitrary choice of delay zero. From Eq. (4) it becomes evident that the measurement-induced delays due to the XUV and the IR beams need to be known, calibrated or removed by measuring with respect to a reference to obtain the target specific delay $\tau_{2q,atom}$ from the measured quantity τ_{2q}.

As discussed in the introduction one possible approach is based on the relative delay between two spatially separated targets. If the measurement-induced changes are the same in both targets, the contribution of the XUV and IR beams cancels out in the delay difference:

$$\Delta\tau_{2q,atom}^{(1)-(2)} = \tau_{2q}^{(1)} - \tau_{2q}^{(2)} = \tau_{2q,atom}^{(1)} - \tau_{2q,atom}^{(2)}. \quad (5)$$

However, as our investigation has demonstrated, the IR phase changes significantly with the target position along the propagation direction across the focus [Fig. 5]. Based on Eq. (4) this dependence will transfer into a time delay according to $\tau_{IR}(z) = \frac{2 \cdot \varphi_{IR}(z)}{2\omega_{IR}}$. This means that any delay comparison of spatially separated targets can potentially introduce an error in $\Delta\tau_{2q,atom}^{(1)-(2)}$ due to uncertainties in the target positions.

In order to evaluate this effect, we calculated the relative delay between our two targets as a function of the position of the second one. Following the earlier analysis [Fig. 4], we can neglect the contribution of the attochirp to the delay difference. Since we used identical gas targets, the relative delay in our case is equal to:

$$\Delta\tau_{2q}^{(1)-(2)}(z) = \tau_{2q}^{(1)} - \tau_{2q}^{(2)}(z) = \frac{2\varphi_{Gouy}^{IR}(z) + \tilde{\varphi}_0}{2\omega_{IR}} = \frac{2\varphi_{Gouy}^{IR}(z)}{2\omega_{IR}} + \tilde{\tau}_0, \quad (6)$$

with $\tilde{\tau}_0$ denoting the remaining constant delay offset. This offset does not depend on the target position and thus will not be considered in the following discussion. Figure 6(a) shows the delay calculated from Eq. (6) that corresponds to the extracted $\varphi_{Gouy}^{IR}(z)$ (blue circles) and a fit with the function $\tau = -B \cdot \tan^{-1}(z/z_R)$, with B = 1.56 ± 0.29 and z_R = 31.3 ± 8.2 mm (red curve). The modulus of the spatial derivative of the fit changes as $\frac{B \cdot z_R}{z_R^2 + z^2}$ and amounts to a maximum of 50 as/mm at the focus [Fig. 6(b)]. This shows clearly that the spatial dependence of the phase along the target interaction region results in a non-negligible contribution to the measured phase and group delay in a RABBITT (or streaking) experiment. Any calibration with spatially separated targets is thus affected by the Gouy phase, which needs to be taken carefully into account. This is particularly important for the case of small differences in photoemission delays, which are of the order of magnitude of a few tens to a few hundreds of attoseconds. Note in case of attosecond streaking, which is not an interferometric technique, the Gouy-phase-induced delay will be half the one measured in the RABBITT.

Optics EXPRESS

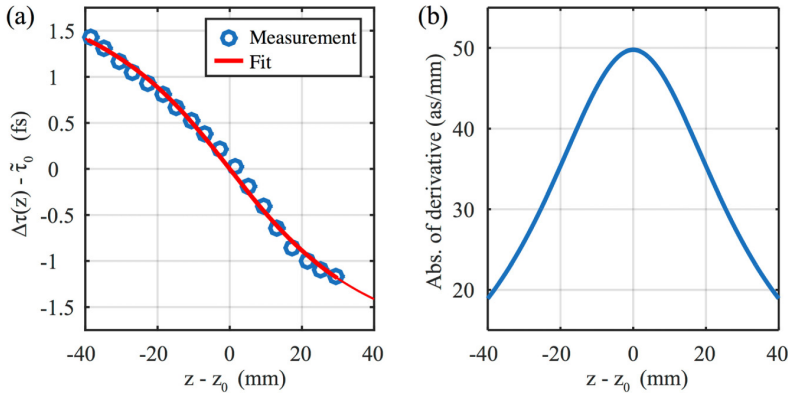

Fig. 6. (a) Relative delay $\Delta\tau_{2q}^{(1)-(2)}(z) = \tau_{2q}^{(1)} - \tau_{2q}^{(2)}(z)$ between simultaneously measured RABBITT traces as a function of the target position in the second target chamber. A constant delay offset $\tilde{\tau}_0$ has been subtracted to obtain a zero delay at the focus. The blue circles are measurement points. The red curve is the result of a fit with the function $\tau = -B \cdot \tan^{-1}(z/z_R)$. (b) Absolute value of the first derivative of the delays in (a) with respect to propagation distance across the focus showing a maximum of 50 as/mm at the focus.

5. Conclusion

In conclusion, we performed a detailed study of the Gouy phase of an annular IR beam, using our two-foci measurement setup in combination with the RABBITT technique. Our results show that the corresponding Gouy phase experiences a shift of more than 2π across the focus, which exceeds by far the π-shift expected for an ideal Gaussian. The Gouy phase contribution still varies significantly even a few centimeters away from the focus. This has two main consequences: (i) in contrast to ideal Gaussian beams, it is not possible to find a spatial region away from the focus where the Gouy phase variation is negligible. Any individual measurement will be affected by the changing IR phase for a detector integrating over the interaction volume. (ii) A spatially dependent IR phase translates into an additional phase or time delay between two spatially separated targets. As in the case of our double foci setup, this applies also to measurements of spatially separated targets within a single focus.

We showed that the effect of the Gouy phase can correspond to additional 50 as/mm time delays around the focus in a RABBITT experiment for our typical beam geometry using a center-hole mirror to collinearly recombine the IR and XUV beams in attosecond pump-probe measurements. If not properly taken into account, this can prevent a reliable calibration and thus the extraction of physical meaningful attosecond delays in photoemission.

Our results show that a precise positioning of the target in the focus is essential for highly accurate time delay measurements. A proper calibration of the Gouy phase of the IR field across the focus together with a suitable choice of the reference target will support better calibration for absolute time delays in attosecond pump-probe measurements using IR and XUV pulses.

Funding

NCCR MUST, funded by the Swiss National Science Foundation (SNSF).